

# The impact of Fc engineering on an anti-CD19 antibody: increased Fc $\gamma$ receptor affinity enhances B-cell clearing in nonhuman primates

Jonathan Zalevsky,<sup>1</sup> Irene W. L. Leung,<sup>1</sup> Sher Karki,<sup>1</sup> Seung Y. Chu,<sup>1</sup> Eugene A. Zhukovsky,<sup>1</sup> John R. Desjarlais,<sup>1</sup> David F. Carmichael,<sup>1</sup> and Chris E. Lawrence<sup>1</sup>

<sup>1</sup>Xencor, Inc, Monrovia, CA

**CD19, a B cell–restricted receptor critical for B-cell development, is expressed in most B-cell malignancies. The Fc-engineered anti-CD19 antibody, XmAb5574, has enhanced Fc $\gamma$  receptor (Fc $\gamma$ R) binding affinity, leading to improved Fc $\gamma$ R-dependent effector cell functions and antitumor activity in murine xenografts compared with the non-Fc-engineered anti-CD19 IgG1 analog. Here, we use XmAb5574 and anti-CD19 IgG1 to further dissect effector cell functions in an im-**

**mune system closely homologous to that of humans, the cynomolgus monkey. XmAb5574 infusion caused an immediate and dose-related B-cell depletion in the blood (to <10% of baseline levels) concomitant with a sustained reduction of natural killer (NK) cells. NK cells had fully recovered by day 15, whereas B-cell recovery was underway by day 57. B cells in secondary lymphoid tissues were depleted (to 34%–61% of vehicle), with involuted germinal centers apparent in the**

**spleen. Anti-CD19 IgG1 had comparable serum exposure to XmAb5574 but demonstrated no B-cell depletion and no sustained NK-cell reduction. Thus, increasing Fc $\gamma$ R binding affinity dramatically increased B-cell clearing. We propose that effector cell functions, possibly those involving NK cells, mediate XmAb5574 potency in cynomolgus monkeys, and that enhancing these mechanisms should advance the treatment of B-cell malignancies in humans. (Blood. 2009;113:3735–3743)**

## Introduction

CD19 is a B cell–restricted signal-transducing cell-surface receptor present on most B cells from the earliest stages of pre-B-cell development until terminal differentiation into plasma cells.<sup>1,2</sup> A critical role for CD19 in B-cell development and activation has been established using CD19-deficient mice. Such mice fail to develop a proper immune response after antigen challenge, exhibit decreased B-cell numbers in the periphery and in lymphoid tissues, lack germinal center (GC) formation, and have decreased serum immunoglobulin (Ig) levels.<sup>1,3,4</sup> Furthermore, anti-CD19 antibodies effectively deplete peripheral B cells in transgenic mice expressing human CD19 and block malignant B-cell growth in murine xenografts.<sup>5–7</sup> With the exception of multiple myeloma,<sup>8</sup> CD19 is expressed in nearly all non-Hodgkin lymphomas and many leukemias.<sup>9,10</sup> Several anti-CD19 antibodies have been evaluated in the clinic for the treatment of such diseases, including unconjugated antibodies,<sup>11,12</sup> antibody–drug conjugates,<sup>13,14</sup> and bispecific antibodies targeting CD19 and CD3.<sup>15,16</sup> Despite the attractiveness of CD19 as an immunotherapeutic target for the treatment of B-cell malignancies, the results with patients have been mixed. Thus, the challenge remains to optimize anti-CD19 antibodies to achieve improved clinical outcome.

The potency of immunotherapeutics depends on multiple mechanisms of action, including those mediated by effector cells expressing Fc $\gamma$  receptors (Fc $\gamma$ Rs).<sup>17</sup> Fc $\gamma$ Rs in turn have activating or inhibitory functional roles and differ in their distribution among effector cells. Monocytes, macrophages, and neutrophils express both activating and inhibitory Fc $\gamma$ Rs, whereas natural killer (NK) cells solely express the activating Fc $\gamma$ RIIIa.<sup>18</sup> Disabling the activating Fc $\gamma$ Rs by deletion of their common  $\gamma$ -chain in mice severely reduced both the B cell–depleting activity of anti-CD20

(rituximab) and the tumor-killing activity of anti-HER-2/neu (trastuzumab).<sup>19,20</sup> Studies of human genetic polymorphisms have demonstrated a relationship between increased Fc $\gamma$ R affinity for the immunotherapeutic and improved clinical outcome. For example, lymphoma and breast cancer patients expressing the higher affinity Fc $\gamma$ RIIIa-158V allele exhibited improved progression-free survival compared with patients expressing the lower affinity 158F allele when treated with rituximab or trastuzumab.<sup>21,22</sup> Together, these human and murine data substantiate the importance of immune effector-mediated mechanisms in the efficacy of immunotherapeutics.

Amino acid- and glyco-engineering of the antibody Fc domain are 2 ways to improve effector cell functions.<sup>23</sup> Fc engineering has improved Fc $\gamma$ R affinity for several antibodies, resulting in significantly enhanced antibody-dependent cell-mediated cytotoxicity (ADCC) and antibody-dependent cell-mediated phagocytosis (ADCP).<sup>24–28</sup> We recently described an Fc-engineered anti-CD19 antibody (XmAb5574) with increased Fc $\gamma$ R binding affinity, which resulted in improved ADCC and ADCP, and increased antitumor efficacy in murine xenografts.<sup>29</sup> Importantly, these functional activities were significantly enhanced relative to the non-Fc-engineered anti-CD19 IgG1 analog (with the same Fv domain as XmAb5574, but retaining the native human IgG1 Fc).

XmAb5574 and anti-CD19 IgG1 are useful tools that permit further elucidation of the contribution of effector cell mechanisms to antibody potency. To date, our knowledge of these mechanisms *in vivo* has been primarily obtained from murine studies. However, extrapolation of murine data to the human setting is constrained both by the extensive use of immunocompromised mice and by the divergent nature of the murine and human immune systems.

Submitted October 1, 2008; accepted December 14, 2008. Prepublished online as *Blood* First Edition paper, December 24, 2008; DOI 10.1182/blood-2008-10-182048.

The publication costs of this article were defrayed in part by page charge

payment. Therefore, and solely to indicate this fact, this article is hereby marked “advertisement” in accordance with 18 USC section 1734.

© 2009 by The American Society of Hematology

Furthermore, one would not use anti-CD19 IgG1 alongside XmAb5574 to study effector cell functions in humans. We think that the nonhuman primate represents the most relevant immune system and accessible test species to dissect the mechanism(s) of effector cell functions and optimize immunotherapeutics for human use. Here, we report that XmAb5574 administration to cynomolgus monkeys caused a dose-dependent, rapid, and extensive clearing of peripheral B cells as well as a reduction of B cells in the lymphoid tissues. A transient reduction in peripheral NK-cell levels concomitant with the maximal rate of B-cell loss was also observed. In contrast, an equal dose of anti-CD19 with the native IgG1 Fc domain had no effect, clearly demonstrating that Fc engineering XmAb5574 for high-affinity binding to Fc $\gamma$ Rs increased the potency of anti-CD19-mediated B-cell depletion.

## Methods

### Antibodies and Fc $\gamma$ Rs

XmAb5574, its IgG1 analog (anti-CD19 IgG1), and an XmAb isotype control antibody (including the same Fc as XmAb5574, but with the Fv from antirespiratory syncytial virus) were generated as described previously.<sup>29</sup> The anti-CD20 antibody rituximab was obtained from RxUSA (Port Washington, NY). Cynomolgus monkey (*Macaca fascicularis*) Fc $\gamma$ R proteins were constructed using gene synthesis as C-terminal His- and GST-fusions based on publicly available sequences (GenBank accession numbers AAL92095 for Fc $\gamma$ RI, AAL92096 for Fc $\gamma$ RIIa, AAL92097 for Fc $\gamma$ RIIb, and AAL92098 for Fc $\gamma$ RIII),<sup>30</sup> expressed in 293T cells, and purified by standard methods.

### Binding to cynomolgus monkey B cells, peripheral lymphocytes, and Fc $\gamma$ Rs

The cynomolgus monkey B-cell line 25136 was a generous gift from Dr Michael McChesney at the University of California, Davis. Cells were incubated with 1  $\mu$ g/mL allophycocyanin (APC)-conjugated antibody J3-119 (APC J3-119; Beckman Coulter, Fullerton, CA) and increasing doses of XmAb5574, anti-CD19 IgG1, or XmAb isotype control antibodies. After a 1-hour incubation, cells were washed and fixed. Binding was measured via flow cytometry using a FACSCanto II (BD Biosciences, San Jose, CA). Dose-response competition curves were fit with a 4-parameter logistic model using SoftmaxPro version 5.2 (Molecular Devices, Sunnyvale, CA) to calculate the 50% inhibitory concentration (IC<sub>50</sub>). IC<sub>50</sub> values are reported as the mean ( $\pm$  SD) of the 4 independent experiments.

Cynomolgus monkey blood was obtained from 5 individual animals (Alpha Genesis, Yemassee, SC) and blocked using an unrelated antibody with the same Fc-engineered changes as XmAb5574 to minimize Fc $\gamma$ R interactions. Blood samples were split; one aliquot was mixed with fluorescein isothiocyanate (FITC)-conjugated XmAb5574 and APC-conjugated anti-CD20 (APC-anti-CD20), and the second aliquot was mixed with FITC-anti-CD19 IgG1 and APC-anti-CD20. After a 2-hour incubation,

red blood cells were lysed, and the samples were washed, fixed, and processed for flow cytometry using a FACSCanto II. Analysis was done by gating onto live lymphocytes, and results were expressed as percentage labeled cells against the total lymphocytes. Two APC-anti-CD20 profiles were collected for each blood sample; the precision for the repeat measures ranged from 0.6% to 1.4% between the 5 samples.

Binding to cynomolgus monkey Fc $\gamma$ Rs was determined using Biacore analysis as described previously for human Fc $\gamma$ Rs.<sup>29</sup>

### Drug treatment and study designs

Cynomolgus monkey studies were conducted at SNBL USA (Everett, WA) according to their standard operating procedures, and all protocols were approved by the SNBL USA Institutional Animal Care and Use Committee. Study designs are described in Table 1. All studies used naive cynomolgus monkeys, 3 to 5 years old and weighing 2.5 to 4.5 kg; animals were acclimated to the study rooms for 21 days before study initiation. XmAb5574 and anti-CD19 IgG1 were formulated in 10 mM sodium phosphate, 150 mM sodium chloride, and 0.01% polysorbate 20 (pH 7.0). Treatments were administered as single 1-hour intravenous infusions to the left saphenous vein.

### Blood and tissue collection and analysis

Blood draws were taken from the cephalic or femoral veins. Samples were collected predose and throughout the duration of each study and processed to serum for bioanalysis or analyzed using flow cytometry for CD20<sup>+</sup>CD3<sup>-</sup> B-cell enumeration, CD20<sup>-</sup>CD3<sup>-</sup> NK-cell enumeration (study 1), and CD16<sup>+</sup>CD3<sup>-</sup> NK-cell enumeration (study 2). The majority of NK cells (> 93% in nonhuman primates) are encompassed by the CD20<sup>-</sup>CD3<sup>-</sup> and CD16<sup>+</sup>CD3<sup>-</sup> populations.<sup>31</sup> Bone marrow aspirate was collected from the humerus before necropsy, and spleen and inguinal lymph node samples were collected after necropsy. All samples were analyzed as per Table 1.

Immunophenotyping was performed on all samples using cynomolgus monkey cross-reactive mouse monoclonal antibodies against CD3, CD16, and CD20 (BD Biosciences). Antibodies were added to the blood sample, incubated, and washed before flow cytometric analysis. Tissue aspirates were minced, strained, and washed before immunostaining. Additional washing steps were included before incubating with anti-CD16 to remove competing XmAb5574. Samples were analyzed on a FACSCalibur flow cytometer (BD Biosciences). Analysis was done by gating onto live lymphocytes and 20 000 events were captured. The absolute counts of the individual lymphocyte populations (CD20<sup>+</sup>CD3<sup>-</sup>, CD20<sup>-</sup>CD3<sup>-</sup>, CD16<sup>+</sup>CD3<sup>-</sup>) were expressed as a percentage of predose baseline. The tissue lymphocyte subpopulations for samples from drug-treated cynomolgus monkeys were expressed as a percentage of the subpopulations derived from those treated with vehicle.

Representative tissue samples of the spleen and lymph node were fixed in 10% neutral buffered formalin and embedded in paraffin. The sectioned tissues were either stained with hematoxylin and eosin or with anti-CD20 (BD Biosciences) and examined using an Olympus BH-2 microscope (Olympus America, Center Valley, PA). Images were captured with a Leica

**Table 1. Cynomolgus monkey studies**

Study no. (treatment)	Duration, days	Dose, mg/kg	No. monkeys (sex)	Necropsy, day(s)	Compartments sampled (FACS)	Analysis
1 (Vehicle)	29	0	4 (2M, 2F)	29	B, S, BM, LN	†
1 (XmAb5574)	29	3	4 (2M, 2F)	29	B, S, BM, LN	†
1 (Anti-CD19 IgG1)	29	3	4 (2M, 2F)	29	B, S, BM, LN	†
2 (Vehicle)	85	0	6 (3M, 3F)	15* and 85	B, BM, LN	‡
2 (XmAb5574)	85	10	6 (3M, 3F)	15* and 85	B, BM, LN	‡

All treatments were given as single 1-hour intravenous infusions.

B indicates blood; S, spleen; BM, bone marrow; and LN, lymph node.

\*One male and one female were necropsied on day 15.

†Analysis for study 1: CD20<sup>+</sup>CD3<sup>-</sup> B cells, CD20<sup>-</sup>CD3<sup>-</sup> NK cells, pharmacokinetics, and antidrug antibody.

‡Analysis for study 2: CD20<sup>+</sup>CD3<sup>-</sup> B cells, CD16<sup>+</sup>CD3<sup>-</sup> NK cells, pharmacokinetics, antidrug antibody, and immunohistochemistry.

DC300 camera using Image Capture Leica IM50 software (Leica Microsystems, Deerfield, IL). Images were processed using Adobe Photoshop version 6.0 (Adobe Systems, San Jose, CA).

### Pharmacokinetic analysis of XmAb5574

Serum bioanalysis was conducted by Prevalere Life Sciences (Whitesboro, NY) using an enzyme-linked immunosorbent assay and appropriate standards and controls to quantify XmAb5574 in cynomolgus monkey serum. The lower limit of quantitation for the method was 20 ng/mL in undiluted monkey serum. This method was suitable to measure both XmAb5574 and anti-CD19 IgG1 in monkey serum. Pharmacokinetic interpretation was conducted using noncompartmental methods computed with WinNonlin 5.20 (Pharsight, Mountain View, CA).

### Antidrug antibody assay

Serum bioanalysis was conducted by Prevalere Life Sciences using an electrochemiluminescent bridging immunoassay method conducted with the MSD platform (Meso Scale Discovery, Gaithersburg, MD).<sup>32</sup> The method uses a floating cutpoint established from naive cynomolgus monkey serum samples; samples that produce signal intensity equal to or greater than the cutpoint are scored positive. The sensitivity of the method, defined as the lowest concentration of positive control antidrug antibody (ADA) that consistently provides electrochemiluminescent signal above the cutpoint, was 31.3 ng/mL in undiluted serum. This method was suitable to detect ADA against both XmAb5574 and anti-CD19 IgG1.

### Serum IgA, IgG, and IgM assay

A simple immunoturbidimetric method was used for the determination of serum IgA, IgG, and IgM. Samples were analyzed on an Olympus AU400 clinical chemistry analyzer (Olympus America).

## Results

The aim of this work was to use the Fc-engineered anti-CD19 antibody XmAb5574 and its non-Fc-engineered analog (anti-CD19 IgG1) to evaluate the mechanistic consequences of Fc engineering on B-cell clearing in an immune system closely homologous to the human.

### XmAb5574 binds to CD19 on cynomolgus monkey B cells and displays enhanced binding to Fc $\gamma$ Rs

Cynomolgus monkeys were used for our studies because they have a similar immune system to humans and have been frequently used in the testing of B-cell modulators (eg, BR3-Fc,<sup>33</sup> anti-CD19,<sup>34</sup> anti-CD20,<sup>35</sup> anti-CD40,<sup>36</sup> anti-CD74,<sup>37</sup> and anti-CD154<sup>38</sup>). Immunohistochemistry is traditionally used to determine the expression of a target antigen and the cross-reactivity to conserved epitopes between human and animal tissues.<sup>39</sup> We found that XmAb5574-specific staining patterns (including cell types stained, subcellular localization, intensity, and frequency) were similar for a panel of 19 cynomolgus monkey and human tissues, including spleen, bone marrow, and inguinal lymph node (data not shown).

To verify this cross-reactivity, we further evaluated XmAb5574 and the anti-CD19 IgG1 analog for binding to cynomolgus monkey CD19 on peripheral blood B cells. A cross-blocking study was done using a cynomolgus monkey B-cell line to measure the binding of XmAb5574, anti-CD19 IgG1, or XmAb isotype control (same Fc as XmAb5574 but with an unrelated Fv) to cell surface CD19 (Figure 1A). XmAb5574 and anti-CD19 IgG1 were equally effective in this study, demonstrating IC<sub>50</sub> values of 13 ( $\pm$  3) and 11 ( $\pm$  2)  $\mu$ g/mL, respectively. Although we did not determine

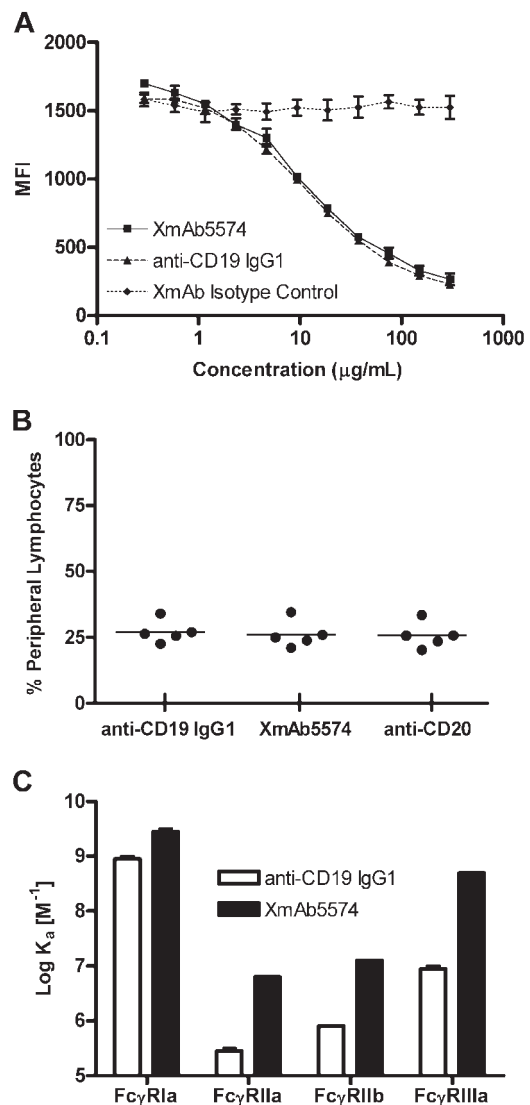


**Figure 1. XmAb5574 binds to cynomolgus monkey CD19 and Fc $\gamma$ Rs.** (A) Binding to a cynomolgus monkey B-cell line was measured with a competitive binding assay. XmAb5574, anti-CD19 IgG1, or XmAb isotype control was used to cross-block binding of 1  $\mu$ g/mL fluorescently conjugated antihuman CD19 monoclonal antibody (clone J3-119). MFI indicates mean fluorescence intensity (in arbitrary units). Results are mean ( $\pm$  range) for duplicate binding curves from a single run and are representative of 4 independent experiments. XmAb5574 and anti-CD19 IgG1 bind equally to cynomolgus monkey CD19. (B) Binding to cynomolgus monkey peripheral blood lymphocytes was assessed using whole blood samples from 5 individual animals. Blood samples were treated with fluorescently conjugated versions of XmAb5574, anti-CD19 IgG1, and anti-CD20 and analyzed by flow cytometry. XmAb5574 and anti-CD19 IgG1 bind CD20<sup>+</sup> lymphocytes. (C) Binding to cynomolgus monkey Fc $\gamma$ Rs was determined using Biacore analysis, and affinities for each Fc $\gamma$ R were plotted as the log of the affinity binding constant K<sub>a</sub>. Results are the mean ( $\pm$  range) of duplicate experiments and demonstrate that XmAb5574 has increased affinity to all Fc $\gamma$ Rs relative to anti-CD19 IgG1; enhancements ranged from 3- to 60-fold, with the largest increase seen for Fc $\gamma$ R1d.

whether XmAb5574 or anti-CD19 IgG1 directly modulate cynomolgus monkey CD19, both antibodies displayed equal caspase-dependent antiproliferative activity against human CD19-expressing cells when crosslinked using antihuman IgG.<sup>29</sup>

To confirm CD19 binding in primary cynomolgus monkey lymphocytes, we obtained whole blood from each of 5 monkeys, treated it with fluorescently conjugated XmAb5574, anti-CD19 IgG1, and the anti-CD20 antibody rituximab, and measured the number of cells bound. XmAb5574 and anti-CD19 IgG1 both bound to the same percentage of lymphocytes as anti-CD20; mean

values ( $\pm$  SD) were 26% ( $\pm$  5%), 27% ( $\pm$  4%), and 26% ( $\pm$  5%), respectively (Figure 1B). Given that B lymphocytes represent a similar percentage of the total lymphocytes in the blood ( $23\% \pm 10\%$ ,  $n = 63$  cynomolgus monkeys), these data indicate that CD19 and CD20 have overlapping expression profiles and that XmAb5574 and anti-CD19 IgG1 bind equally to cynomolgus monkey B cells.

The Fc region of XmAb5574 contains 2 mutations (S239D and I332E) that increase affinity for human Fc $\gamma$ Rs.<sup>29</sup> In preparation for our monkey studies, it was important to determine the affinities of XmAb5574 and anti-CD19 IgG1 for cynomolgus monkey Fc $\gamma$ Rs so that we could better interpret the *in vivo* results. Although cynomolgus monkeys are routinely used for toxicologic and pharmacologic evaluation of Fc $\gamma$ R-engaging immunotherapeutics, the Fc $\gamma$ Rs of this species are less well characterized than those from mouse or human. The amino acid sequence identities between cynomolgus monkey and human receptors are 92%, 89%, 89%, and 91% for the Fc $\gamma$ RI, Fc $\gamma$ RIIa, Fc $\gamma$ RIIb, and Fc $\gamma$ RIIIa sequences, respectively (G. Lazar, unpublished observations, September 20, 2005)<sup>40</sup>; this high degree of sequence similarity suggested that the binding affinities might also be similar. The extracellular portions of the cynomolgus monkey Fc $\gamma$ Rs were expressed as recombinant fusion proteins, purified, and used in Biacore-binding studies to determine their association with XmAb5574 and anti-CD19 IgG1. Fc engineering increased the binding of XmAb5574 to cynomolgus monkey Fc $\gamma$ RI, Fc $\gamma$ RIIa, Fc $\gamma$ RIIb, and Fc $\gamma$ RIIIa by 3-, 25-, 16-, and 60-fold, respectively, compared with the anti-CD19 IgG1 analog (Figure 1C). The binding affinities of anti-CD19 IgG1 for cynomolgus monkey Fc $\gamma$ Rs were similar to those previously observed for human Fc $\gamma$ Rs, and the degree of affinity enhancements obtained with XmAb5574 were comparable with those obtained for human Fc $\gamma$ Rs.<sup>29</sup>

Taken together, these results confirm the cynomolgus monkey as an appropriate species for studying the effects of XmAb5574 and anti-CD19 IgG1.

#### XmAb5574 enhances B-cell depletion in blood and lymphoid tissues compared with the anti-CD19 IgG1 analog

To investigate the impact of Fc $\gamma$ R binding on B-cell depletion, we compared the ability of XmAb5574 and anti-CD19 IgG1 to deplete cynomolgus monkey B cells. Cynomolgus monkeys were given a single intravenous infusion of XmAb5574 or anti-CD19 IgG1 (both at 3 mg/kg), or vehicle, and followed for 29 days (Table 1). XmAb5574 caused a rapid and substantial clearing of peripheral B cells (CD20<sup>+</sup>CD3<sup>-</sup>), dropping to 30% of predose baseline levels 24 hours after administration and reaching a nadir of 6% on day 22. In contrast, animals treated with anti-CD19 IgG1 were indistinguishable from vehicle controls (Figure 2A). Similar results were seen in lymphoid tissues, with XmAb5574-mediated B-cell depletion at day 29 being greatest in spleen (remaining B cells were 39% of vehicle), followed by bone marrow and lymph node (50% and 66% of vehicle, respectively; Figure 2B). Again, anti-CD19 IgG1 had no effect on tissue B cells. To confirm that the apparent clearing of CD20<sup>+</sup>CD3<sup>-</sup> B cells was not the result of reduced surface expression of CD20, samples were also probed with a second B-cell marker, CD40. In cynomolgus monkeys, CD20 and CD40 have a highly overlapping expression pattern on CD3<sup>-</sup> B cells in the blood, spleen, and lymph nodes.<sup>41</sup> The CD40<sup>+</sup>CD3<sup>-</sup> results duplicated those with CD20<sup>+</sup>CD3<sup>-</sup> (data not shown).

The serum concentrations of XmAb5574 and anti-CD19 IgG1 were examined to determine whether the different B-cell clearing effects between the 2 could be attributed to differences in exposure.

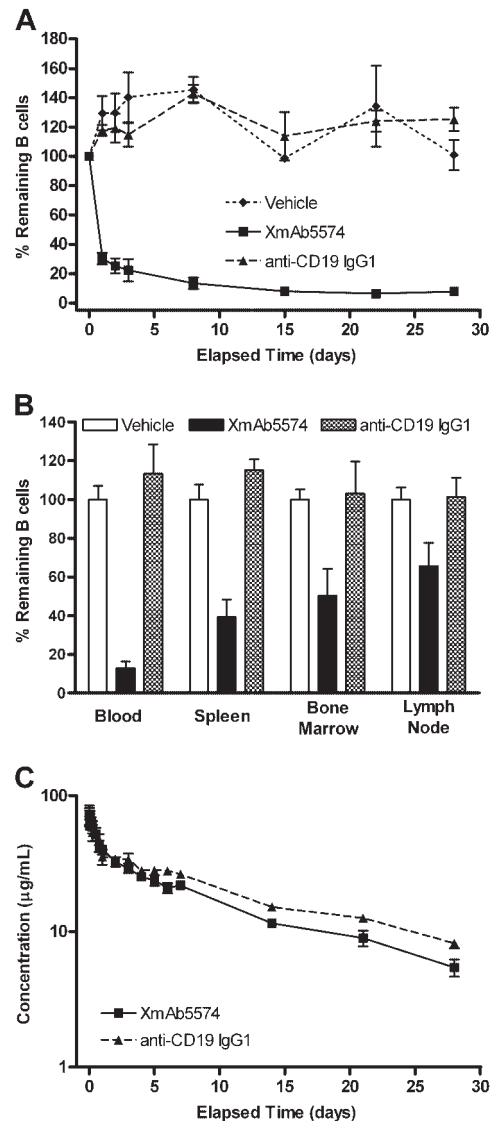


**Figure 2. XmAb5574 but not anti-CD19 IgG1 depletes B cells in the blood and tissue.** XmAb5574, anti-CD19 IgG1, or vehicle was administered as a single 3-mg/kg infusion (4 cynomolgus monkeys per treatment group). B cells were measured in the blood throughout the study (A) and in the blood, bone marrow, spleen, and lymph node on study conclusion, 29 days later (B). B-cell levels were assessed using flow cytometry with a CD20<sup>+</sup>CD3<sup>-</sup> gate and expressed as the percentage of baseline (mean  $\pm$  SE). XmAb5574 caused a substantial reduction in blood and tissue B cells, whereas anti-CD19 IgG1 was indistinguishable from vehicle. The rank order of depletion was blood > spleen > bone marrow > lymph node. (C) Serum concentrations of XmAb5574 and anti-CD19 IgG1 were measured using an immunoassay and are shown on a log-linear plot (mean  $\pm$  SD of 4 animals). The half-lives were 11 ( $\pm$  1) and 13 ( $\pm$  2) days for XmAb5574 and anti-CD19 IgG1, respectively, demonstrating that these antibodies displayed similar exposure and pharmacokinetic properties with the given dosing regimen.

After intravenous infusion, both antibodies cleared from serum in a biphasic manner (Figure 2C). XmAb5574 and anti-CD19 IgG1 had comparable distribution and elimination, indicating that the superior B-cell clearing effect of XmAb5574 was not the result of increased exposure. The calculated half-lives were 11 ( $\pm$  1) days and 13 ( $\pm$  2) days for XmAb5574 and anti-CD19 IgG1, respectively. ADA screening was conducted to determine whether ADA was affecting the pharmacokinetics or pharmacodynamics of the 2 antibodies. The results showed that 2 of 4 XmAb5574- and 1 of 4 anti-CD19 IgG1-treated animals mounted a weak antidrug immune response. However, ADA did not appear to alter the clearance of either antibody or inhibit the B-cell depletion induced by

XmAb5574. These results suggest that the enhanced B-cell depletion seen with XmAb5574 is probably the result of its increased affinity for cynomolgus monkey Fc $\gamma$ Rs compared with non-Fc-engineered anti-CD19 IgG1.

#### XmAb5574-induced B-cell depletion is followed by recovery in blood and lymphoid tissues

The second cynomolgus monkey study evaluated the pharmacodynamic effects of XmAb5574 after a single intravenous infusion at 10 mg/kg (Table 1). XmAb5574 again caused an immediate and substantial reduction of peripheral B cells, dropping to 22% of predose baseline levels 24 hours after administration and reaching a nadir of 5% on day 15 (Figure 3A). This was a more rapid and extensive B-cell depletion than was observed at 3 mg/kg, indicating a dose-dependent effect. Recovery was underway in all 4 remaining

monkeys by day 57 (reaching 30% of baseline), and by study end at day 85, peripheral B cells had returned to 78% of baseline levels.

At day 15, extensive depletion of B cells occurred in the bone marrow and lymph node of the XmAb5574-treated cynomolgus monkeys relative to those treated with vehicle (Figure 3B). B-cell levels dropped to 18% and 35% of vehicle, respectively, for bone marrow and lymph node, and recovered to 37% and 84% by day 85. Again, the magnitude of B-cell depletion in the tissues was greater than with 3 mg/kg.

Studies using human CD19 transgenic<sup>+/-</sup> mice revealed that a single injection of antihuman CD19 caused extensive B-cell depletion and significantly reduced serum IgA, IgG, and IgM levels for more than 10 weeks.<sup>7</sup> We evaluated serum Ig levels during the course of the study and found them unchanged compared with baseline and vehicle-treated cynomolgus monkeys, despite the substantial clearing of peripheral and GC B cells (Figure 3C for IgG, data not shown for IgA and IgM).

#### XmAb5574-induced involution in spleen germinal centers is followed by recovery

The GC microenvironment, present in the spleen and lymph nodes, is the main source of memory B cells and plasma cells that produce high-affinity antibodies. Mice deficient in CD19 fail to produce GCs or exhibit a normal immune response after antigen challenge.<sup>42</sup> Consequently, we evaluated the cellular composition and architecture of splenic tissue sections using histology and CD20 immunohistochemistry. XmAb5574 at 10 mg/kg caused a loss of the typical compact cellularity (Figure 4B,D) and CD20 immunostaining (Figure 4A,C) in the spleen GCs at day 15, resulting in an involuted morphology. The splenic GC phenotype observed after XmAb5574 treatment was similar to that seen for other B cell-depleting antibodies<sup>35</sup> and was consistent with our flow cytometric B-cell depletion results. By day 85, the involuted GCs in the spleen were no longer present, and the morphology and CD20 immunostaining returned to that observed for vehicle-treated controls.

#### XmAb5574 transiently reduces peripheral blood NK cells concomitant with B-cell clearing

NK cells were enumerated by CD20<sup>-</sup>CD3<sup>-</sup> and CD16<sup>+</sup>CD3<sup>-</sup> subset analysis in the cynomolgus monkey studies (Table 1). Both immunoprofiling methods were needed to validate the results because NK cells have been shown to modulate CD16 (Fc $\gamma$ RIIIa) expression after antibody engagement.<sup>43</sup> XmAb5574, anti-CD19 IgG1 (both at 3 mg/kg), and vehicle caused a rapid reduction of peripheral blood CD20<sup>-</sup>CD3<sup>-</sup> NK cells (to 37%, 63%, and 57% of individual predose baselines, respectively) 24 hours after administration (Figure 5A). Levels returned to baseline after 48 hours in the vehicle- and anti-CD19 IgG1-treated controls. This short-lived drop in NK cells seen in both control groups may represent a stress response to infusion and handling, despite a 3-week predose acclimation period. No B-cell clearing was evident in either control group (Figure 2A). In contrast, NK-cell reduction was sustained in the XmAb5574-treated animals and did not recover completely until day 15. The observed NK-cell reduction was coincident with the peripheral B-cell depletion induced by XmAb5574 (Figure 2A).

Similar results were seen at the 10 mg/kg dose of XmAb5574 (Figure 5B). Peripheral blood CD16<sup>+</sup>CD3<sup>-</sup> NK cells were extensively reduced 24 hours after administration (32% of baseline vs 78% for vehicle-treated controls), and this reduction was sustained for a much longer period than the vehicle-treated group, which rapidly recovered to near baseline levels 72 hours after dosing.

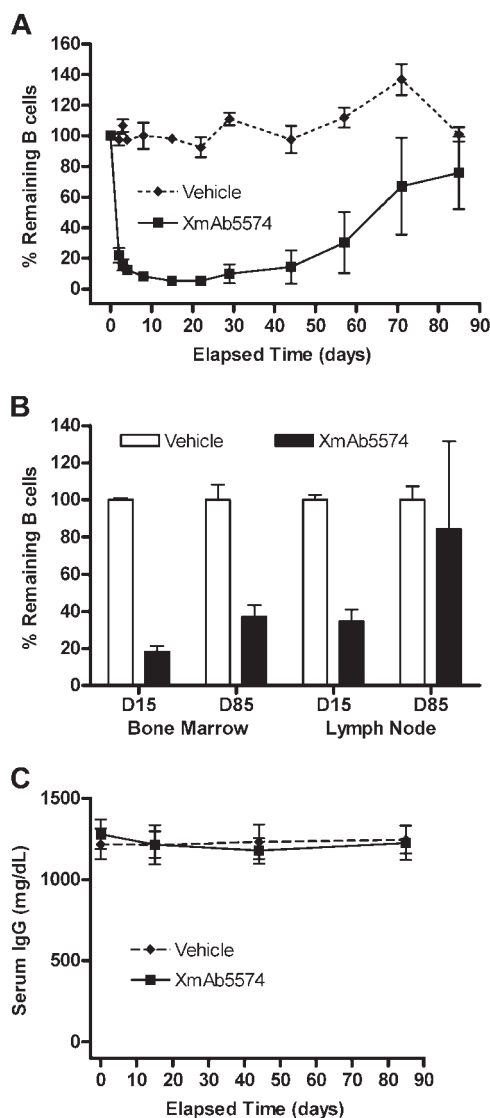


**Figure 3. XmAb5574-induced depletion is followed by B-cell recovery in blood and tissue.** XmAb5574 was given as a single infusion at 10 mg/kg to 6 cynomolgus monkeys. B cells were measured in the blood throughout the study and in the bone marrow and lymph node tissues on days 15 and 85 (D15 and D85) by the method described in the Figure 2 legend. (A) Blood B-cell levels dropped rapidly before the onset of recovery, which was underway in all animals by day 57. (B) B-cell levels in the tissue were reduced at day 15 and were recovering at day 85. (C) Serum IgG remained unchanged throughout the study despite extensive B-cell depletion. Values shown are the mean ( $\pm$  SE) at each time point.

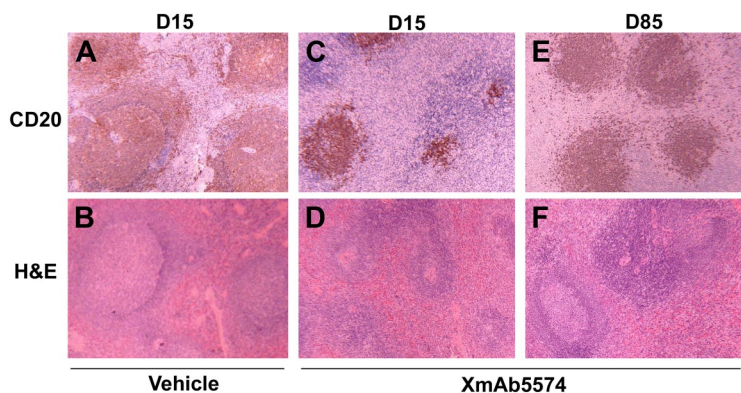


**Figure 4. XmAb5574 caused reversible involution of germinal centers in the spleen.** Spleen tissue was collected 15 and 85 days (D15 and D85) after administration of either vehicle (A,B) or 10 mg/kg XmAb5574 (C-F). Tissue sections were stained either for CD20 (B-cell immunostain) or with hematoxylin and eosin (H&E) for tissue morphology as indicated. The CD20 immunostained area (brown-stained cells) was decreased by XmAb5574 (C) in comparison to vehicle control (A), and this was associated with germinal center involution (B,D). CD20 immunostaining (E) and germinal center morphology (F) had recovered to baseline levels at day 85. For all panels, sections were examined using an Olympus BH-2 microscope equipped with a 60 $\times$ /0.17 NA objective. Images were captured with a Leica DC300 camera using Image Capture Leica IM50 software and processed with Adobe Photoshop version 6.0.

Again, the maximum fall in peripheral B-cell depletion (Figure 3A) occurred during the period of NK-cell reduction. Given that both NK-cell enumeration methods (CD20<sup>-</sup>CD3<sup>-</sup> and CD16<sup>+</sup>CD3<sup>-</sup>) produced equivalent results, these data suggest that NK cells may be involved in XmAb5574-mediated B-cell clearing in cynomolgus monkeys.

## Discussion

We have Fc-engineered a humanized anti-CD19 antibody to increase Fc $\gamma$ R binding affinities with the aim of enhancing its therapeutic activity against B-cell malignancies. The resultant antibody (XmAb5574) and the non-Fc-engineered analog (anti-

CD19 IgG1) are critical tools permitting the study of effector cell mechanisms on antibody potency in a highly relevant immune system, the cynomolgus monkey. In summary, we highlight, for the first time, (1) binding affinities of humanized antibodies for cynomolgus monkey Fc $\gamma$ Rs, (2) direct comparison in cynomolgus monkeys of an Fc-engineered anti-CD19 antibody with increased Fc $\gamma$ R affinity versus its IgG1 analog, (3) extensive B-cell clearing in cynomolgus monkeys by an unconjugated Fc-engineered anti-CD19 antibody, and (4) the concomitant reduction in peripheral NK cells, suggesting their possible involvement in this B-cell clearing. We hereby propose that Fc engineering is able to enhance effector cell mechanisms and thus improve antibody potency in a highly relevant immune system.

XmAb5574 caused a dose-dependent and reversible clearing of peripheral B cells in cynomolgus monkeys. B cells were depleted more readily in the blood compared with the tissue compartments. This differential effect in blood versus tissues has also been demonstrated with other B cell-depleting antibodies (anti-BR3, anti-CD20, anti-CD40, anti-CD74, and anti-CD154), given the caveats that different agents, dosing regimens, and species of nonhuman primates were used.<sup>33-38,41,44-46</sup> Importantly, B-cell depletion has not been reported for either of the anti-CD19 antibody drug conjugates evaluated in cynomolgus monkeys.<sup>34,47</sup> Our anti-CD19 IgG1 was similarly ineffective in cynomolgus monkeys, but Fc engineering the antibody to increase Fc $\gamma$ R affinity was clearly able to cause almost total B-cell depletion.

Unconjugated therapeutic antibodies generally function through 3 mechanisms: complement-mediated cytotoxicity, cell surface receptor-mediated signaling, and involvement of effector cell functions. Failure to engage any one or a combination of these could explain the poor activity of anti-CD19 IgG1. Anti-CD19 IgG1 binds cynomolgus monkey CD19 equally to XmAb5574; and although we cannot rule out a complement-mediated effect in vivo, both antibodies failed to induce complement activity in vitro,<sup>29</sup> and the S239D/I332E substitutions did not alter the inherent complement activity of other antibodies (J.R.D., unpublished observations, December 1, 2008).<sup>25</sup> Clearly, the S239D/I332E substitutions in the Fc region are solely responsible for the increased potency of XmAb5574. The importance of Fc $\gamma$ R affinity in mediating B-cell clearing is supported by anti-CD20 data. Anti-CD20 IgG1 has been reported to effectively clear peripheral B cells in nonhuman primates, whereas anti-CD20 IgG4 has no effect, even though the non-Fc-dependent activities are identical for both antibodies.<sup>45</sup> Because IgG4 and IgG1 differ in their affinity and selectivity profile for human Fc $\gamma$ Rs,<sup>39</sup> it is highly probable that the B-cell clearing observed with both anti-CD20 IgG1 and XmAb5574 is a

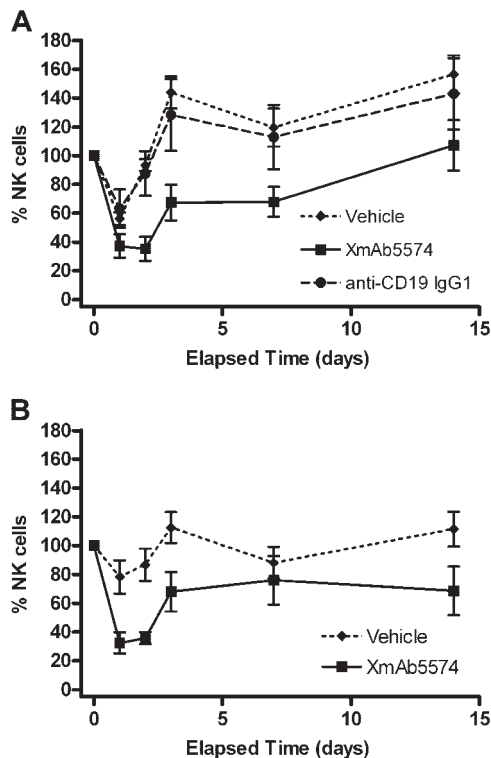


**Figure 5. XmAb5574 gave a sustained reduction in NK-cell levels in blood compared with vehicle or anti-CD19 IgG1.** XmAb5574 administration at either 3 mg/kg (A) or 10 mg/kg (B) produced a substantial and sustained drop in NK-cell levels with recovery beginning by day 4 and complete by day 15. Vehicle and anti-CD19 IgG1 treatment also reduced NK-cell levels after administration, but the levels quickly recovered to baseline by days 2 to 3. NK cells were measured using flow cytometry with a gate for CD20<sup>-</sup>CD3<sup>-</sup> (A) or CD16<sup>+</sup>CD3<sup>-</sup> (B) and are expressed as a percentage of baseline. Values shown are the mean ( $\pm$  SE) at each time point.

consequence of improved Fc $\gamma$ R affinity relative to their anti-CD20 IgG4 and anti-CD19 IgG1 analogs.

The inactivity of anti-CD19 IgG1 could also be explained by low antibody exposure. Infusion at 3 mg/kg yielded a maximum serum concentration of approximately 80  $\mu$ g/mL; nevertheless, it is possible that higher or repeated dosing resulting in significantly higher maximum serum concentrations could induce B-cell clearing. In addition, the overall serum concentration-versus-time profiles for XmAb5574 and its IgG1 analog were similar, with no significant differences among the computed pharmacokinetic parameters, demonstrating that Fc engineering of XmAb5574 did not affect the pharmacokinetic properties relative to the nonengineered antibody.

We investigated the effect of anti-CD19 IgG1 and XmAb5574 on cynomolgus monkey serum Ig levels because the requirement for CD19 in B-cell maturation, class switching, positive selection, and differentiation into immunoglobulin secreting plasmablasts and plasma cells has to date only been demonstrated in the mouse.<sup>48</sup> Serum IgG, IgA, and IgM levels were reduced in mice treated with anti-CD19.<sup>7</sup> In contrast, we found no change in these immunoglobulins throughout the course of our 85-day cynomolgus monkey study, despite the substantial XmAb5574-mediated clearing of blood and tissue B cells. Corroborating our data, anti-CD20 treatment of nonhuman primates did not reduce plasma cell levels in secondary lymphoid tissues even in the face of extensive B-cell clearing.<sup>35,44</sup> The sparing of plasma cells and the preservation of serum Ig levels are a beneficial property and support continued development of XmAb5574.

We observed a transient reduction in CD20<sup>-</sup>CD3<sup>-</sup> and CD16<sup>+</sup>CD3<sup>-</sup> cells concomitant with the peripheral B-cell clearing, allowing us to speculate which Fc $\gamma$ Rs and effector cell type(s) propagate the Fc-dependent functions of XmAb5574. Significant evidence implicates NK cells because of their Fc $\gamma$ R profile, abundance in peripheral blood, and professional cellular cytotoxicity functions. Unlike other effector cells, such as monocytes and neutrophils, which express a variety of Fc $\gamma$ Rs, NK cells solely express the activating Fc $\gamma$ RIIIa. Indeed, XmAb5574 has been engineered to have substantially increased Fc $\gamma$ RIIIa affinity relative to anti-CD19 IgG1. NK cells outnumber B cells in the human circulation by 3 to 1<sup>49</sup>; and in our cynomolgus monkey studies, we observed approximately 3 NK cells (CD20<sup>-</sup>CD3<sup>-</sup>) for every 2 B cells (CD20<sup>+</sup>CD3<sup>-</sup>). In clinical studies, the effectiveness of rituximab was improved by coadministration of recombinant interleukin-2, which has been shown to activate NK cells, enhance NK-cell survival, replenishment, and cytotoxic function, and promote their margination and trafficking from the circulation.<sup>50-52</sup> In cynomolgus monkeys, rituximab elicited a dose-dependent decrease in CD16<sup>+</sup>CD3<sup>-</sup> NK cells in the blood, which correlated with the degree of B-cell clearing.<sup>25</sup> Clinical therapy with rituximab, the anti-HLA-DR antibody apolizumab, or recombinant interleukin-2 also caused a transient reduction of circulating NK cells,<sup>43,52</sup> and it was suggested that NK-cell activation could lead to their margination and trafficking from the circulation.<sup>52</sup> Similarly, our results showed that the S239D/I332E substitutions in XmAb5574 increased B-cell clearing and induced a more pronounced and prolonged NK-cell drop than the ineffective anti-CD19 IgG1. These and other studies using higher affinity Fc $\gamma$ RIIIa allele-expressing NK cells demonstrate a positive correlation between antibody affinity for Fc $\gamma$ RIIIa and enhanced cellular activation,<sup>43,52,54</sup> and indicate that increasing Fc $\gamma$ RIIIa affinity could maximize therapeutic efficacy more than simply elevating doses of antibody. Although we cannot rule out other effector cell types or

other antibody-mediated effects, such as complement activation, the correlation between reduced NK-cell levels and the maximal rate of B-cell depletion suggests that NK cells may play a role in XmAb5574-induced peripheral B-cell clearing.

The mechanism of antibody-induced B-cell depletion in the tissues is poorly understood and rarely documented. Tissue B-cell depletion could be affected by antibody exposure, the difference in total B-cell number between the blood and tissue compartments, and the diverse nature of the effector cells present in the tissues. Although we did not measure tissue antibody levels, we expect blood concentrations to be higher than in tissues after direct intravenous infusion. The blood compartment contains approximately 2% of the total lymphocyte pool<sup>55</sup> and is exposed to the greatest concentration of XmAb5574. Our studies showed dose-dependent tissue B-cell depletion, and we predict that further increased dose levels or repeat administration would result in even greater tissue B-cell depletion. It is unclear which effector cell types could mediate XmAb5574-induced B-cell depletion in lymphoid tissues because they contain few Fc $\gamma$ RIIIa-expressing NK cells.<sup>56</sup> Murine studies have revealed an important role for macrophages in antibody-induced cytotoxicity.<sup>57</sup> In cynomolgus monkeys, diverse effector cells, such as macrophages (spleen), Kupffer cells (liver), and dendritic cells (lymph node), could mediate the depletion. Such effector cells express the full profile of Fc $\gamma$ Rs. Recently, increased affinity for Fc $\gamma$ RIIIa has been shown to enhance macrophage function.<sup>26</sup> XmAb5574 exhibits increased ADCP *in vitro*<sup>29</sup> and has enhanced cynomolgus monkey Fc $\gamma$ RIIIa affinity, suggesting it may also have improved effector cell function in the tissue microenvironment. In addition, tissue-dependent effects, such as interaction with the stroma and the presence of B-cell survival factors coupled with the more heterogeneous B-cell population, may negatively impact the sensitivity and susceptibility of tissue B cells to XmAb5574. Alternatively, others have hypothesized that B-cell depletion is an active process in the circulation and that the apparent tissue depletion is a consequence of the inability to replenish B cells from the blood compartment.<sup>58-60</sup> It is important to note that rituximab, despite its failure to completely clear cynomolgus monkey tissue B cells, continues to be a highly effective treatment for many B-cell malignancies.

Through our studies, we have substantiated a relationship between Fc $\gamma$ R affinity and B-cell clearing in cynomolgus monkeys. The work validates a rationale and a highly relevant test system to accelerate the development and evaluate the potency of effector function-enhanced immunotherapeutics in preparation for clinical studies. We anticipate that future studies with Fc-engineered antibodies will facilitate the elucidation of effector cell mechanisms and optimize the design of immunotherapeutics with tailored functions.

## Acknowledgments

The authors thank Greg Lazar and David Szymkowski for providing critical comments, Marie Ary for preparation of the manuscript, study director Stefan Nechev and the entire staff at SNBL USA for conducting and supporting the *in vivo* studies, principal investigator Deborah Candido and the entire staff at Prevalere Life Sciences for serum bioanalysis, and Dan Combs for conducting pharmacokinetic interpretation.

## Authorship

Contribution: C.E.L., J.Z., S.Y.C., E.A.Z., S.K., I.W.L.L., J.R.D., and D.F.C. designed the research; S.Y.C., I.W.L.L., and S.K. performed the research and collected data; C.E.L., J.Z.,

S.K., and S.Y.C. interpreted and analyzed the data; and C.E.L. and J.Z. drafted the manuscript. All authors reviewed and approved the final version.

Conflict-of-interest disclosure: The authors are Xencor employees.

Correspondence: Jonathan Zalevsky, Xencor, Inc, 111 West Lemon Ave, Monrovia, CA 91016; e-mail: jzalevsky@xencor.com.

## References

- Sato S, Steeber DA, Jansen PJ, Tedder TF. CD19 expression levels regulate B lymphocyte development: human CD19 restores normal function in mice lacking endogenous CD19. *J Immunol*. 1997;158:4662-4669.
- Tedder TF, Inaoki M, Sato S. The CD19-CD21 complex regulates signal transduction thresholds governing humoral immunity and autoimmunity. *Immunity*. 1997;6:107-118.
- Engel P, Zhou LJ, Ord DC, Sato S, Koller B, Tedder TF. Abnormal B lymphocyte development, activation, and differentiation in mice that lack or overexpress the CD19 signal transduction molecule. *Immunity*. 1995;3:39-50.
- Otero DC, Anzelon AN, Rickert RC. CD19 function in early and late B cell development: I. Maintenance of follicular and marginal zone B cells requires CD19-dependent survival signals. *J Immunol*. 2003;170:73-83.
- Ghetie MA, Picker LJ, Richardson JA, Tucker K, Uhr JW, Vitetta ES. Anti-CD19 inhibits the growth of human B-cell tumor lines in vitro and of Daudi cells in SCID mice by inducing cell cycle arrest. *Blood*. 1994;83:1329-1336.
- Pietersz GA, Wenjun L, Sutton VR, et al. In vitro and in vivo antitumor activity of a chimeric anti-CD19 antibody. *Cancer Immunol Immunother*. 1995;41:53-60.
- Yazawa N, Hamaguchi Y, Poe JC, Tedder TF. Immunotherapy using unconjugated CD19 monoclonal antibodies in animal models for B lymphocyte malignancies and autoimmune disease. *Proc Natl Acad Sci U S A*. 2005;102:15178-15183.
- Ishikawa H, Tsuyama N, Mahmoud MS, et al. CD19 expression and growth inhibition of tumors in human multiple myeloma. *Leuk Lymphoma*. 2002;43:613-616.
- Anderson KC, Bates MP, Slaughenhaupt BL, Pinkus GS, Schlossman SF, Nadler LM. Expression of human B cell-associated antigens on leukemias and lymphomas: a model of human B cell differentiation. *Blood*. 1984;63:1424-1433.
- Ginaldi L, De Martinis M, Matutes E, Farahat N, Morilla R, Catovsky D. Levels of expression of CD19 and CD20 in chronic B cell leukaemias. *J Clin Pathol*. 1998;51:364-369.
- Hekman A, Honselaar A, Vuist WM, et al. Initial experience with treatment of human B cell lymphoma with anti-CD19 monoclonal antibody. *Cancer Immunol Immunother*. 1991;32:364-372.
- Vlasveld LT, Hekman A, Vyth-Dreese FA, et al. Treatment of low-grade non-Hodgkin's lymphoma with continuous infusion of low-dose recombinant interleukin-2 in combination with the B-cell-specific monoclonal antibody CLB-CD19. *Cancer Immunol Immunother*. 1995;40:37-47.
- Grossbard ML, Lambert JM, Goldmacher VS, et al. Anti-B4-blocked ricin: a phase I trial of 7-day continuous infusion in patients with B-cell neoplasms. *J Clin Oncol*. 1993;11:726-737.
- Uckun FM, Messinger Y, Chen CL, et al. Treatment of therapy-refractory B-lineage acute lymphoblastic leukemia with an apoptosis-inducing CD19-directed tyrosine kinase inhibitor. *Clin Cancer Res*. 1999;5:3906-3913.
- Bargou R, Leo E, Zugmaier G, et al. Tumor regression in cancer patients by very low doses of a T cell-engaging antibody. *Science*. 2008;321:974-977.
- Molhoj M, Crommer S, Brischwein K, et al. CD19/CD3-bispecific antibody of the BiTE class is far superior to tandem diabody with respect to redirected tumor cell lysis. *Mol Immunol*. 2007;44:1935-1943.
- Cohen-Solal JF, Cassard L, Fridman WH, Sautes-Fridman C. Fc $\gamma$  receptors. *Immunol Lett*. 2004;92:199-205.
- Robertson MJ, Ritz J. Biology and clinical relevance of human natural killer cells. *Blood*. 1990;76:2421-2438.
- Clynes RA, Towers TL, Presta LG, Ravetch JV. Inhibitory Fc receptors modulate in vivo cytotoxicity against tumor targets. *Nat Med*. 2000;6:443-446.
- Uchida J, Hamaguchi Y, Oliver JA, et al. The innate mononuclear phagocyte network depletes B lymphocytes through Fc receptor-dependent mechanisms during anti-CD20 antibody immunotherapy. *J Exp Med*. 2004;199:1659-1669.
- Cartron G, Dacheux L, Salles G, et al. Therapeutic activity of humanized anti-CD20 monoclonal antibody and polymorphism in IgG Fc receptor Fc $\gamma$ RIIIa gene. *Blood*. 2002;99:754-758.
- Musolino A, Naldi N, Bortesi B, et al. Immunoglobulin G fragment C receptor polymorphisms and clinical efficacy of trastuzumab-based therapy in patients with HER-2/neu-positive metastatic breast cancer. *J Clin Oncol*. 2008;26:1789-1796.
- Desjarlais JR, Lazar GA, Zhukovsky EA, Chu SY. Optimizing engagement of the immune system by anti-tumor antibodies: an engineer's perspective. *Drug Discov Today*. 2007;12:898-910.
- Bowles JA, Wang SY, Link BK, et al. Anti-CD20 monoclonal antibody with enhanced affinity for CD16 activates NK cells at lower concentrations and more effectively than rituximab. *Blood*. 2006;108:2648-2654.
- Lazar GA, Dang W, Karki S, et al. Engineered antibody Fc variants with enhanced effector function. *Proc Natl Acad Sci U S A*. 2006;103:4005-4010.
- Richards JO, Karki S, Lazar GA, Chen H, Dang W, Desjarlais JR. Optimization of antibody binding to Fc $\gamma$ RIIIa enhances macrophage phagocytosis of tumor cells. *Mol Cancer Ther*. 2008;7:2517-2527.
- Shields RL, Namenuk AK, Hong K, et al. High resolution mapping of the binding site on human IgG1 for Fc $\gamma$ RI, Fc $\gamma$ RII, Fc $\gamma$ RIII, and FcRn and design of IgG1 variants with improved binding to the Fc $\gamma$ R. *J Biol Chem*. 2001;276:6591-6604.
- Stavenhagen JB, Gorlatov S, Tuailon N, et al. Fc optimization of therapeutic antibodies enhances their ability to kill tumor cells in vitro and controls tumor expansion in vivo via low-affinity activating Fc $\gamma$  receptors. *Cancer Res*. 2007;67:8882-8890.
- Horton HM, Bennett MJ, Pong E, et al. Potent in vitro and in vivo efficacy of an Fc-engineered anti-CD19 monoclonal antibody against lymphoma and leukemia. *Cancer Res*. 2008;68:8049-8057.
- National Center for Biotechnology Information, GenBank. Accessed September 20, 2005.
- Webster RL, Johnson RP. Delineation of multiple subpopulations of natural killer cells in rhesus macaques. *Immunology*. 2005;115:206-214.
- Moxness M, Tatarewicz S, Weeraratne D, et al. Immunogenicity testing by electrochemiluminescent detection for antibodies directed against therapeutic human monoclonal antibodies. *Clin Chem*. 2005;51:1983-1985.
- Vugmeyster Y, Seshasayee D, Chang W, et al. A soluble BAFF antagonist, BR3-Fc, decreases peripheral blood B cells and lymphoid tissue marginal zone and follicular B cells in cynomolgus monkeys. *Am J Pathol*. 2006;168:476-489.
- Messinger Y, Yanishevski Y, Ek O, et al. In vivo toxicity and pharmacokinetic features of B43 (anti-CD19)-genistein immunoconjugate in non-human primates. *Clin Cancer Res*. 1998;4:165-170.
- Schroder C, Azimzadeh AM, Wu G, Price JO, Atkinson JB, Pierson RN. Anti-CD20 treatment depletes B-cells in blood and lymphatic tissue of cynomolgus monkeys. *Transpl Immunol*. 2003;12:19-28.
- Kelley SK, Gelzleichter T, Xie D, et al. Preclinical pharmacokinetics, pharmacodynamics, and activity of a humanized anti-CD40 antibody (SGN-40) in rodents and non-human primates. *Br J Pharmacol*. 2006;148:1116-1123.
- Stein R, Mattes MJ, Cardillo TM, et al. CD74: a new candidate target for the immunotherapy of B-cell neoplasms. *Clin Cancer Res*. 2007;13[suppl]:5556s-5563s.
- Brams P, Black A, Padlan EA, et al. A humanized anti-human CD154 monoclonal antibody blocks CD154-CD40 mediated human B cell activation. *Int Immunopharmacol*. 2001;1:277-294.
- Loisel S, Ohresser M, Pallardy M, et al. Relevance, advantages and limitations of animal models used in the development of monoclonal antibodies for cancer treatment. *Crit Rev Oncol Hematol*. 2007;62:34-42.
- Nimmerjahn F, Ravetch JV. Fc $\gamma$  receptors: old friends and new family members. *Immunity*. 2006;24:19-28.
- Vugmeyster Y, Beyer J, Howell K, et al. Depletion of B cells by a humanized anti-CD20 antibody PRO70769 in *Macaca fascicularis*. *J Immunother*. 2005;28:212-219.
- Rickert RC, Rajewsky K, Roes J. Impairment of T-cell-dependent B-cell responses and B-1 cell development in CD19-deficient mice. *Nature*. 1995;376:352-355.
- Bowles JA, Weiner GJ. CD16 polymorphisms and NK activation induced by monoclonal antibody-coated target cells. *J Immunol Methods*. 2005;304:88-99.
- Alwayn IP, Xu Y, Basker M, et al. Effects of specific anti-B and/or anti-plasma cell immunotherapy on antibody production in baboons: depletion of CD20- and CD22-positive B cells does not result in significantly decreased production of anti- $\alpha$ -Gal antibody. *Xenotransplantation*. 2001;8:157-171.
- Reff ME, Carner K, Chambers KS, et al. Depletion of B cells in vivo by a chimeric mouse human monoclonal antibody to CD20. *Blood*. 1994;83:435-445.
- Lin WY, Gong Q, Seshasayee D, et al. Anti-BR3 antibodies: a new class of B-cell immunotherapy combining cellular depletion and survival blockade. *Blood*. 2007;110:3959-3967.
- Uckun FM, Yanishevski Y, Tumer N, et al. Pharmacokinetic features, immunogenicity, and toxicity of B43(anti-CD19)-pokeweed antiviral protein immunotoxin in cynomolgus monkeys. *Clin Cancer Res*. 1997;3:325-337.



48. Wang Y, Carter RH. CD19 regulates B cell maturation, proliferation, and positive selection in the FDC zone of murine splenic germinal centers. *Immunity*. 2005;22:749-761.
49. Caligiuri MA. Human natural killer cells. *Blood*. 2008;112:461-469.
50. Eisenbeis CF, Grainger A, Fischer B, et al. Combination immunotherapy of B-cell non-Hodgkin's lymphoma with rituximab and interleukin-2: a pre-clinical and phase I study. *Clin Cancer Res*. 2004;10:6101-6110.
51. Gluck WL, Hurst D, Yuen A, et al. Phase I studies of interleukin (IL)-2 and rituximab in B-cell non-Hodgkin's lymphoma: IL-2 mediated natural killer cell expansion correlations with clinical response. *Clin Cancer Res*. 2004;10:2253-2264.
52. Meropol NJ, Barresi GM, Fehniger TA, Hitt J, Franklin M, Caligiuri MA. Evaluation of natural killer cell expansion and activation in vivo with daily subcutaneous low-dose interleukin-2 plus periodic intermediate-dose pulsing. *Cancer Immunol Immunother*. 1998;46:318-326.
53. Congy-Jolivet N, Bolzec A, Ternant D, Ohresser M, Watier H, Thibault G. Fc $\gamma$ RIIIa expression is not increased on natural killer cells expressing the Fc $\gamma$ RIIIa-158V allotype. *Cancer Res*. 2008;68:976-980.
54. Varchetta S, Gibelli N, Oliviero B, et al. Elements related to heterogeneity of antibody-dependent cell cytotoxicity in patients under trastuzumab therapy for primary operable breast cancer over-expressing Her2. *Cancer Res*. 2007;67:11991-11999.
55. Trepel F. Number and distribution of lymphocytes in man: a critical analysis. *Klin Wochenschr*. 1974;52:511-515.
56. Freud AG, Caligiuri MA. Human natural killer cell development. *Immunol Rev*. 2006;214:56-72.
57. Tedder TF, Baras A, Xiu Y. Fc $\gamma$  receptor-dependent effector mechanisms regulate CD19 and CD20 antibody immunotherapies for B lymphocyte malignancies and autoimmunity. *Springer Semin Immunopathol*. 2006;28:351-364.
58. Glennie MJ, French RR, Cragg MS, Taylor RP. Mechanisms of killing by anti-CD20 monoclonal antibodies. *Mol Immunol*. 2007;44:3823-3837.
59. Gong Q, Ou Q, Ye S, et al. Importance of cellular microenvironment and circulatory dynamics in B cell immunotherapy. *J Immunol*. 2005;174:817-826.
60. Vugmeyster Y, Howell K, Bakshi A, Flores C, Hwang O, McKeever K. B-cell subsets in blood and lymphoid organs in *Macaca fascicularis*. *Cytometry A*. 2004;61:69-75.